



Fang Yu M.D., Carlos Bazan M.D., Bundhit Tantiwongkosi M.D.

University of Texas Health Science Center San Antonio
University Hospital
Department of Radiology



3D IMAGING IN MULTIPLE SCLEROSIS

Introduction

- Multiple sclerosis is a chronic inflammatory demyelinating condition of the central nervous system (CNS).
- Afflicts millions of individuals worldwide
 - **Leading non-traumatic cause of neurological disability in young adults** (Yousem DM, 2010).
- Clinical MRI has seen extensive application in initial diagnosis as well as disease monitoring given its sensitivity for detecting CNS lesions.

Introduction

- Continued efforts to refine the diagnostic criteria for multiple sclerosis.
 - Increased emphasis on T₂/FLAIR hyperintense lesions.
- **Dissemination in time and space** are key features of the disorder as defined by the McDonald Criteria
 - Can be determined based on clinical exam **and** imaging findings (Polman CH, 2010).

Introduction

- To meet MRI criteria for **dissemination in space (DIS)**, there must be at least one T2 lesion in 2 of the 4 following locations:
 - Periventricular
 - Infratentorial
 - Juxtacortical
 - Spinal cord
- **Dissemination in time (DIT)** by MRI criteria may be met by either:
 - New T2 or gadolinium-enhancing lesion on follow-up MRI, regardless of time from baseline imaging
 - Simultaneous presence of enhancing and nonenhancing lesions at any time.

Introduction

- 3D spatial encoding may be obtained by adding phase encoding along a third orthogonal axis with respect to conventional 2D planar imaging.
- Advantages of 3D compared to 2D MR acquisitions include:
 - ↑ **signal-to-noise ratio (SNR)**, as signal is obtained from more hydrogen atoms (thick slab/volume versus a single planar slice)
 - ↑ spatial (through-plane) resolution
 - Ability to reconstruct images in different orientations from the same dataset (Mugler JP 3rd, 2000).

Introduction

- These qualities make 3D MRI ideal for the diagnosis, as well as follow-up care in MS, in lieu of improved lesion detection.
 - However, a **prohibitive limitation has been the increased acquisition time** compared to 2D sequences.
- Fortunately, recent advances in MR technology, including high performance gradient and receiver systems, **has led to the development of clinically practical 3D volume acquisition techniques**.
 - While gradient echo sequences are now routinely utilized for this purpose, fast spin echo sequences (FSE) are well suited for T₂ weighted imaging.

Introduction


- For a **2D FSE** sequence, the scan time is determined by: $\frac{TR \times N_{PE1} \times NSA}{ETL}$ (McRobbie DW, 2003).
 - TR is the repetition time
 - N_{PE1} represents the number of phase encoding steps
 - NSA is the number of averages
 - ETL is the echo train length or turbo factor
- The scan time for **3D FSE** can be determined by incorporating the number of phase encoding steps in the third dimension (N_{PE2}):
$$\frac{TR \times N_{PE1} \times N_{PE2} \times NSA}{ETL}$$

Introduction

- 2D-FLAIR demonstrates excellent sensitivity in identifying supratentorial lesion, **but is less effective in evaluating the posterior fossa.**
- **Double inversion recovery** utilizes two 180-degree inversion recovery pulses to attenuate the CSF as well as white matter signal (Redpath TW, 1994).
 - A 180-degree inversion pulse is followed by an inversion time (TI_1), a 2nd 180-degree inversion pulse followed by a second shorter inversion time (TI_2), and then the rest of the sequence.
- Recent studies suggest that **DIR may be better able to elucidate mixed grey-white matter as well as infratentorial lesions.**



Introduction

- Project Aims:
 - Compare 3D FLAIR and DIR with conventional 2D FLAIR on a 3T MRI system in the detection and characterization of MS lesions.
 - Compare 3D FLAIR and 3D DIR with each other on a 3T MRI system in the detection and characterization of MS lesions.
- 

Methods

- Approval was obtained from our Internal Review Board.
 - 6 MS patients were referred from Neurology Department.
 - 4 non-MS patients were also imaged.
 - All 10 patients received 2D FLAIR imaging - 9 of these received 3D FLAIR, and 6 also underwent 3D DIR.
- A radiologist reviewed the images after they were transferred to a desktop workstation (Fuji PACS).
 - Manual regions of interest (ROIs) were drawn, & the mean normalized signal and area (mm²) were recorded.

Methods

- MR examinations were performed on a 3T Philips Achieva system using a standard 8-element phase array SENSE (sensitivity encoding) head coil. Parameters are shown below:

Parameter	3D DIR	3D FLAIR	2D FLAIR
FOV (mm)	250	250	240
Matrix	208 x 208	224 x 224	320 x 184
Acquired voxel (mm)	1.2/1.2/1.3	1.12/1.12/1.12	0.75/1.3/4
SENSE factor	2	2.6	None
Turbo Factor	173	182	31
Repetition time (ms)	5500	4800	11000
Echo time (ms)	252	279	125
Inversion time (ms)	2600/625	1650	2800
Number of signals averaged	2	2	1
Acquisition time	6:30	4:52	3:40

Methods

- Lesions were recorded with respect to their location:
 - Juxtacortical, grey-white matter, deep white matter, periventricular, infratentorial, or other (e.g. deep grey nuclei).

- Contrast ratios were calculated for each lesion:

$$\frac{SI_1 - SI_2}{SI_1 + SI_2}$$

- SI_1 represents the signal intensity within the lesion (region) of interest, while SI_2 represents the signal intensity in normal appearing white matter (NAWM).
- Statistical significance was determined using a 2-tail student t-test, with indeterminate variance.

Results: Lesions by location

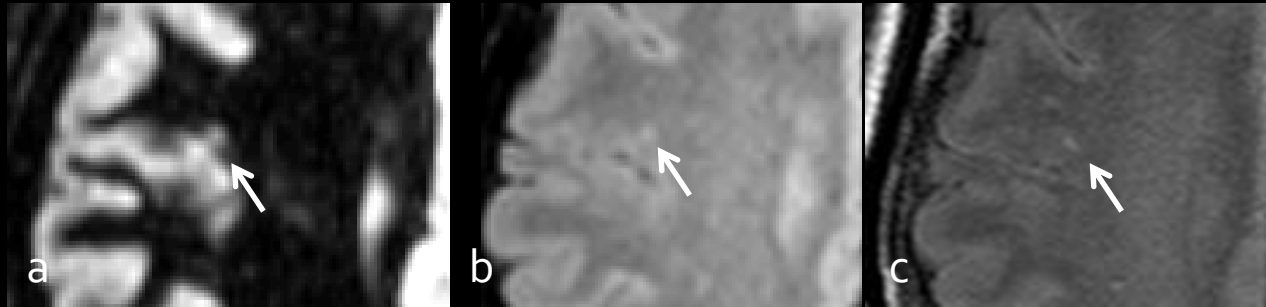


Figure 1: Axial 3D DIR (a), 3D FLAIR (b), and 2D FLAIR (c) demonstrate a hyperintense **juxtacortical** lesion



Figure 2: Axial 3D DIR (a), 3D FLAIR (b), and 2D FLAIR (c) demonstrate a hyperintense lesion situated at the **grey matter-white matter** border

Results: Lesions by location

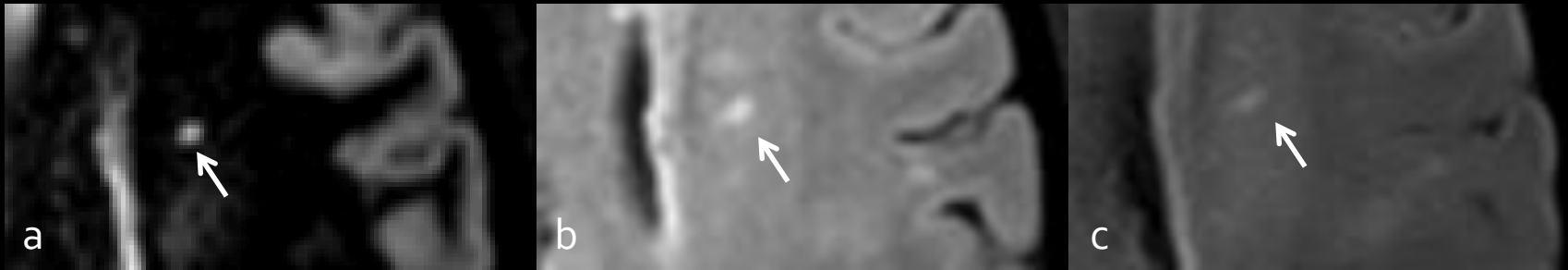


Figure 3: Axial 3D DIR (a), 3D FLAIR (b), and 2D FLAIR (c) demonstrate a hyperintense lesion situated in the **deep white matter**

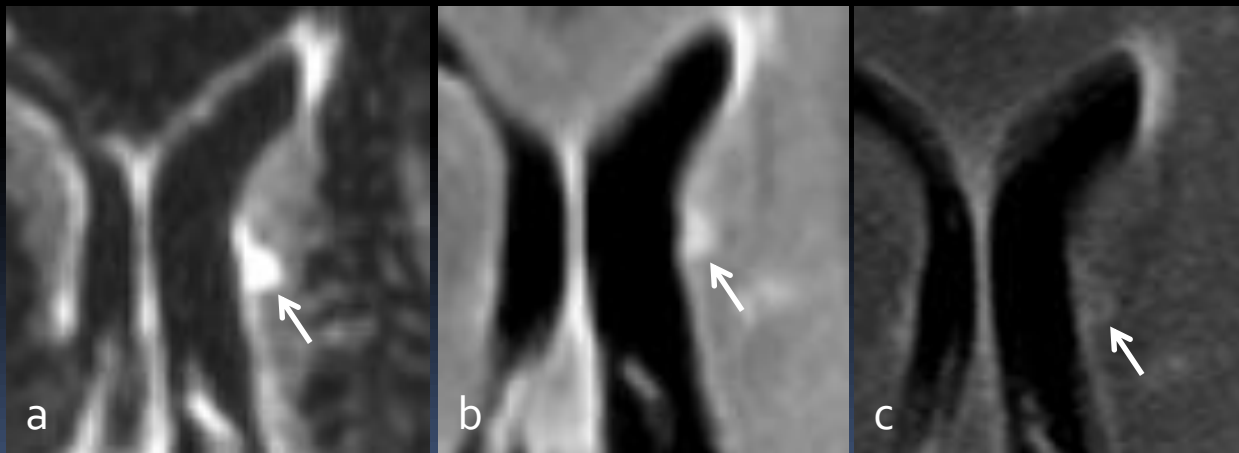
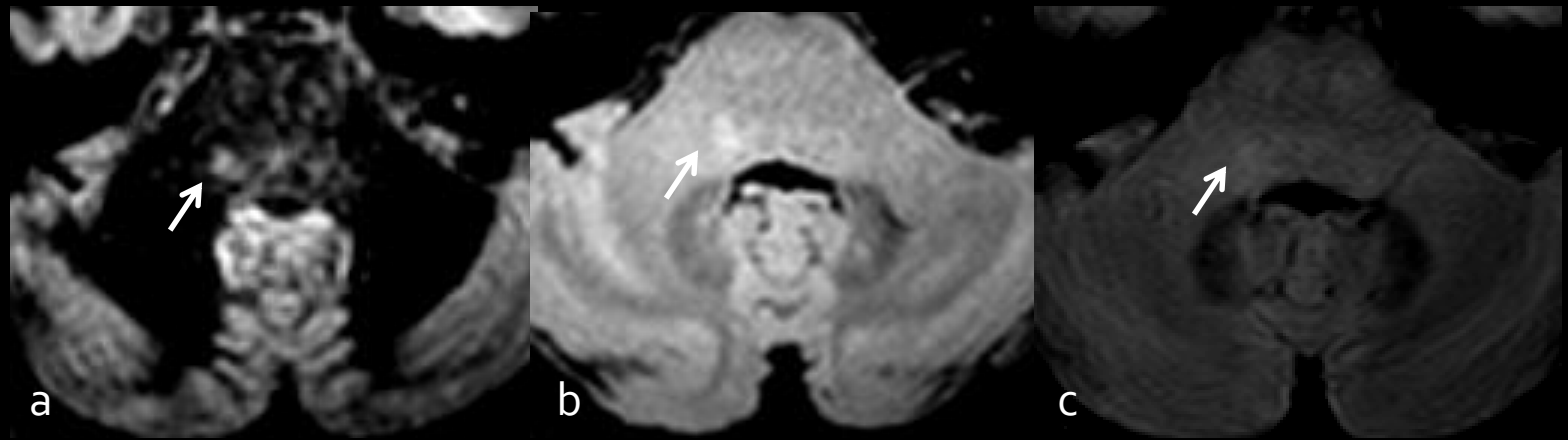


Figure 4: Axial 3D DIR (a), 3D FLAIR (b), and 2D FLAIR (c) demonstrate a hyperintense lesion **abutting the left lateral ventricle (periventricular)**.

Results: Lesions by location



Axial 3D DIR (a), 3D FLAIR (b), and 2D FLAIR (c) demonstrate a hyperintense **infratentorial** lesion.

Results: 3D & 2D FLAIR

From the results of 9 patients, **3D FLAIR was superior to 2D FLAIR in lesion detection** in all locations (32% increase detection rate overall [428 compared to 323 lesions]).

Lesions (All)	Total	GM-WM	Periventricular	Deep WM	Juxtacortical	Other	Infratentorial
3D FLAIR	428	26	69	242	59	10	22
2D FLAIR	323	14	56	193	46	5	9
% Difference	32.51	85.71	23.21	25.39	28.26	100.00	144.44

Furthermore, **the lesions were also more conspicuous ($p < 0.05$) on 3D FLAIR**, as indicated by the increased contrast ratio.

Contrast ratios (All)	GM-WM	Periventricular	Deep WM	Juxtacortical	Other	Infratentorial
3D FLAIR	0.25	0.31	0.25	0.25	0.32	0.27
2D FLAIR	0.15	0.22	0.17	0.18	0.11	0.17
p-value	4.33E-03	6.84E-07	2.08E-13	1.31E-03	5.90E-03	4.92E-04

Lesion size did not differ significantly.

Lesion area (mm ²) (All)	GM-WM	Periventricular	Deep WM	Juxtacortical	Other	Infratentorial
3D FLAIR	9.06	20.62	9.40	10.35	7.80	12.85
2D FLAIR	10.19	22.46	9.56	10.29	9.68	14.56
p-value	0.10	0.70	0.86	0.98	0.22	0.73

Results: 3D & 2D FLAIR

Among **MS** patients (n = 6), the trend for increased lesion detection persisted in all locations (29% increase detection rate overall [266 versus 206 lesions]).

Lesions (MS)	Total	GM-WM	Periventricular	Deep WM	Juxtacortical	Other	Infratentorial
3D FLAIR	266	19	38	147	43	5	14
2D FLAIR	206	10	35	118	35	3	5
% Difference	29.13	90.00	8.57	24.58	22.86	66.67	180.00

Likewise, the lesions remained more conspicuous ($p < 0.05$).

Contrast ratios (MS)	GM-WM	Periventricular	Deep WM	Juxtacortical	Other	Infratentorial
3D FLAIR	0.33	0.49	0.31	0.31	0.48	0.40
2D FLAIR	0.21	0.31	0.17	0.20	0.13	0.19
p-value	1.29E-03	2.86E-08	2.00E-29	1.46E-05	5.21E-03	5.21E-04

Lesion size did not differ significantly between sequences, although tended to be larger in the MS-only group.

Lesion area (mm ²) (MS)	GM-WM	Periventricular	Deep WM	Juxtacortical	Other	Infratentorial
3D FLAIR	10.83	34.40	10.85	12.41	9.94	18.46
2D FLAIR	12.66	33.07	11.38	12.18	11.30	22.32
p-value	5.98E-01	7.23E-01	8.77E-01	6.87E-01	2.84E-01	5.34E-01

Results: 3D DIR & 2D FLAIR

From the results of all 7 patients, 3D DIR was also superior to 2D FLAIR in lesion detection in all locations (36% increase detection rate overall [275 compared to 202 lesions]). This was particularly notable for GM-WM and infratentorial lesions.

Lesions	Total	GM-WM	Periventricular	Deep WM	Juxtacortical	Other	Infratentorial
3D DIR	275	21	45	150	41	5	13
2D FLAIR	202	10	33	124	26	2	7
% Difference	36.14	110.00	36.36	20.97	57.69	150.00	85.71

Lesions were also more conspicuous ($p < 0.05$) on 3D DIR, as indicated by the increased contrast ratio.

Contrast ratios	GM-WM	Periventricular	Deep WM	Juxtacortical	Other	Infratentorial
3D DIR	0.82	0.77	0.65	0.74	0.80	0.80
2D FLAIR	0.15	0.20	0.14	0.14	0.08	0.18
p-value	5.05E-20	2.32E-40	9.82E-97	2.43E-38	3.71E-02	9.25E-10

Lesions did not differ significantly in size.

Lesion area (mm ²)	GM-WM	Periventricular	Deep WM	Juxtacortical	Other	Infratentorial
3D DIR	6.24	30.82	5.95	6.90	6.52	14.15
2D FLAIR	5.93	42.03	6.59	7.15	7.25	19.49
p-value	0.88	0.51	0.33	0.89	0.66	0.64

Results: 3D DIR & 2D FLAIR

Among **MS** patients (n = 5), increased lesion detection held up in all locations (36% increase detection rate overall [166 compared to 122 lesions]. This was most significant in the GM-WM and infratentorial locations.

Lesions (MS)	Total	GM-WM	Periventricular	Deep WM	Juxtacortical	Infratentorial
3D DIR	166	16	30	76	36	8
2D FLAIR	122	8	21	67	22	4
% Difference	36.07	100.00	42.86	13.43	63.64	100.00

The lesions remained more conspicuous ($p < 0.05$).

Contrast ratios (MS)	GM-WM	Periventricular	Deep WM	Juxtacortical	Infratentorial
3D DIR	0.84	0.81	0.73	0.75	0.84
2D FLAIR	0.16	0.22	0.13	0.14	0.17
p-value	2.38E-02	2.18E-25	2.03E-82	4.74E-33	6.08E-01

Again, lesion size did not differ significantly between sequences, although they tended to be smaller in DIR.

Lesion area (mm ²) (MS)	GM-WM	Periventricular	Deep WM	Juxtacortical	Infratentorial
3D DIR	6.43	42.23	5.40	7.03	19.40
2D FLAIR	5.99	61.26	6.17	7.21	29.25
p-value	0.73	0.46	0.35	0.93	0.61

Results: 3D DIR & 3D FLAIR

From the results of all 6 patients, 3D DIR did **not** differ significantly from 3D FLAIR in overall lesion detection. However, with regards to lesion location, there was a notable **increase in detection of GM-WM lesions with DIR**.

Lesions	Total	GM-WM	Periventricular	Deep WM	Juxtacortical	Infratentorial
3D DIR	235	18	34	141	33	9
3D FLAIR	232	11	34	147	32	8
% Difference	1.29	63.64	0.00	-4.08	3.13	12.50

The lesions had **increased contrast ratio ($p < 0.05$) on 3D DIR**. However, the signal intensity was increased on 3D FLAIR (1447.1 compared to 798.3 [$p < 0.05$]).

Contrast ratios	GM-WM	Periventricular	Deep WM	Juxtacortical	Infratentorial
3D DIR	0.81	0.74	0.64	0.72	0.77
3D FLAIR	0.19	0.27	0.18	0.18	0.23
p-value	3.36E-13	3.94E-31	1.25E-86	7.77E-31	6.41E-09

Lesions did not differ significantly in size.

Lesion area (mm ²)	GM-WM	Periventricular	Deep WM	Juxtacortical	Infratentorial
3D DIR	5.34	7.04	5.61	4.61	6.70
3D FLAIR	5.76	7.12	6.39	5.84	7.53
p-value	0.56	0.70	0.19	0.35	0.32

Results: 3D DIR & 3D FLAIR

As expected, in the MS group (n = 4), 3D DIR did **not** differ significantly from 3D FLAIR in overall lesion detection. DIR maintained an **lead in detection of GM-WM lesions**, but detected slightly fewer deep WM lesions

Lesions (MS)	Total	GM-WM	Periventricular	Deep WM	Juxtacortical	Infratentorial
3D DIR	131	13	19	67	28	4
3D FLAIR	130	8	19	72	27	4
% Difference	0.77	62.50	0.00	-6.94	3.70	0.00

Lesions had **increased contrast ratio (p<0.05) on 3D DIR**. However, signal intensity was greater with 3D FLAIR (1508.7 compared to 894.3 [p<0.05]).

Contrast ratios (MS)	GM-WM	Periventricular	Deep WM	Juxtacortical	Infratentorial
3D DIR	0.84	0.79	0.72	0.72	0.80
3D FLAIR	0.23	0.32	0.22	0.18	0.30
p-value	7.19E-11	3.21E-21	2.23E-61	9.75E-25	1.53E-04

Lesions did not differ significantly in size, although tended to be smaller on DIR.

Lesion area (mm ²) (MS)	GM-WM	Periventricular	Deep WM	Juxtacortical	Infratentorial
3D DIR	5.22	6.28	4.61	4.36	7.88
3D FLAIR	6.04	6.66	5.49	5.64	8.95
p-value	0.45	0.57	0.13	0.39	0.52

Discussion

- Through our analysis, we demonstrated superior MS lesion detection with 3D compared to conventional 2D MR sequences.
- This advantage applied to both supra- as well as infratentorial lesions.
 - An additional advantage of 3D imaging that was not evaluated in our study was decreased reliance on patient head positioning, which often limits follow-up comparisons.
- We also found that 3D FLAIR and DIR did not differ substantially in overall lesion detection.
- In lieu of existing guidelines, including McDonald Criteria, **we recommend the utilization of 3D imaging (either FLAIR or DIR) for routine MS work-up.**

Discussion

- 3D FLAIR had a higher SNR (higher signal intensity albeit lower contrast ratio), less sensitivity to CSF pulsation artifacts, and a shorter acquisition time (4.9 to 6.5 minutes) compared to 3D DIR.
 - In this context, we currently favor utilizing 3D FLAIR over DIR in routine practice.
- With that said, 3D DIR was more effective in detecting mixed grey-white lesions.
 - This may aid in disease monitoring, and add prognostic value in light of growing appreciation for the clinical impact of grey-matter involvement in MS (Calabrese M, 2009).
 - Future investigations will help to elucidate the role of cortical lesion detection in clinical management.

Limitations

- The primary limitations of our study was the relatively small sample size and lack of long term follow-up.
- Goals for the future include:
 - Continued imaging of new patients, as well as follow-up of those who were included in the current analysis.
 - This may be extended to therapeutic trials.
 - Regression analyses for various MS phenotypes (primary progressive versus relapsing remitting and secondary progressive MS).

Citations

- Calabrese M, R. M. (2009). Cortical lesions in primary progressive multiple sclerosis: a 2-year longitudinal MR study. *Neurology*, 72, 1330-6.
- Geurts JJ, P. P. (2005, July). Intracortical lesions in multiple sclerosis: improved detection with 3D double inversion-recovery MR imaging. *Radiology*, 236(1).
- Grossman RI, G. J. (1994, March). Magnetization transfer: theory and clinical applications in neuroradiology. *Radiographics*, 14(2), 279-90.
- McRobbie DW, M. E. (2003). *MRI from Picture to Proton*. Cambridge, England: Cambridge University Press.
- Mugler JP 3rd, B. S. (2000). Optimized single-slab three-dimensional spin-echo MR imaging of the brain. *Radiology*, 216(3), 891-9.
- Polman CH, R. S.-W. (2010, February). Diagnostic criteria for multiple sclerosis: 2010 revisions to the McDonald criteria. *Ann Neurol*, 69(2), 292-302.
- Redpath TW, S. F. (1994). Technical note: use of a double inversion recovery pulse sequence to image selectively gray and white matter. *Br J Radiol*, 64, 1258-63.
- Turetschek K, W. P. (1998). Double inversion recovery imaging of the brain: initial experience and comparison with fluid attenuated inversion recovery imaging. *Magn Reson Imaging*, 16, 127-35.
- Wattjes MP, L. G. (2007, January). Double inversion recovery brain imaging at 3T: diagnostic value in the detection of multiple sclerosis lesions. *AJNR Am J Neuroradiol.*, 28(1), 54-9.
- Yousem DM, Z. R. (2010). *Neuroradiology: The Requisites* (Vol. 3). Philadelphia, PA: Elsevier Health Sciences.



Special thanks

- Rebecca Romero, M.D. – Assistant professor of neurology, MS specialist
 - Wilson Altmeyer, M.D. – Assistant professor of radiology, Neuroradiology section
 - Timothy Duong, Ph.D. – Professor, Research Imaging Institute
 - Gilbert Cortez – MRI technician
 - Carmen Young – IRB nurse
- 